Nuclear Engineering and Technology 49 (2017) 1495–1504

Contents lists available at ScienceDirect

Nuclear Engineering and Technology

journal homepage: www.elsevier.com/locate/net

Original Article

Implications of using a 50-μm-thick skin target layer in skin dose coefficient calculation for photons, protons, and helium ions

Yeon Soo Yeom, Thang Tat Nguyen, Chansoo Choi, Min Cheol Han, Hanjin Lee, Haegin Han, Chan Hyeong Kim*

Department of Nuclear Engineering, Hanyang University, 17 Haengdang, Seongdong, Seoul 133–791, Republic of Korea

ARTICLE INFO

Article history:
Received 4 December 2016
Received in revised form
21 January 2017
Accepted 4 June 2017
Available online 13 June 2017

Keywords:
ICRP Reference Voxel Phantom
Monte Carlo
Polygonal-Mesh
Skin Dose Coefficient
Skin Target Layer

ABSTRACT

In a previous study, a set of polygon-mesh (PM)-based skin models including a 50-μm-thick radiosensitive target layer were constructed and used to calculate skin dose coefficients (DCs) for idealized external beams of electrons. The results showed that the calculated skin DCs were significantly different from the International Commission on Radiological Protection (ICRP) Publication 116 skin DCs calculated using voxel-type ICRP reference phantoms that do not include the thin target layer. The difference was as large as 7,700 times for electron energies less than 1 MeV, which raises a significant issue that should be addressed subsequently. In the present study, therefore, as an extension of the initial, previous study, skin DCs for three other particles (photons, protons, and helium ions) were calculated by using the PM-based skin models and the calculated values were compared with the ICRP-116 skin DCs. The analysis of our results showed that for the photon exposures, the calculated values were generally in good agreement with the ICRP-116 values. For the charged particles, by contrast, there was a significant difference between the PM-model-calculated skin DCs and the ICRP-116 values. Specifically, the ICRP-116 skin DCs were smaller than those calculated by the PM models—which is to say that they were underestimated—by up to ~16 times for both protons and helium ions. These differences in skin dose also significantly affected the calculation of the effective dose (E) values, which is reasonable, considering that the skin dose is the major factor determining effective dose calculation for charged particles. The results of the current study generally show that the ICRP-116 DCs for skin dose and effective dose are not reliable for charged particles.

1. Introduction

Computational human phantoms, coupled with Monte Carlo radiation transport codes, play an important role in calculation of organ and effective dose coefficients (DCs) resulting from ionizing radiation exposures. Currently, voxel-type computational phantoms, representing organs and tissues as an assembly of tiny 3D cuboids, are the most popular [1]. Constructed based on tomographic images [e.g., computed tomographic (CT) images] of real persons, voxel phantoms are anatomically more realistic than the previously used mathematical (or stylized) phantoms, the organs and tissues of which are represented by simple quadric surface equations such as ellipsoids, elliptical cylinders, and cones. Acknowledging the advantages of voxel phantoms, the International Commission on Radiological Protection (ICRP) adopted a set of adult male and female voxel phantoms as the ICRP reference adult phantoms [2].

However, voxel phantoms still have limitations in representing thin or small organs and tissues, due mainly to the limited, generally millimeter-scale, voxel sizes [3–16]. Skin is one of the representative thin organs that cannot be properly represented in voxel phantoms. Fig. 1, for example, shows the skins of the ICRP reference voxel phantoms viewed in the superior-inferior direction, revealing that they are discontinuous, having a considerable amount of holes. This problem leads to distortion of calculated dose values not only for the skin, but also for neighbor organs and tissues, particularly for weakly penetrating radiations [17]. ICRP Publication 116 [18], for instance, reports that breast doses resulting from isotropic (ISO) proton irradiation are overestimated by up to ~100 times at 1 MeV, because some protons directly deposit energies to the breasts through the holes in the skin of the ICRP voxel

* Corresponding author.
E-mail address: chkim@hanyang.ac.kr (C.H. Kim).

http://dx.doi.org/10.1016/j.net.2017.06.002

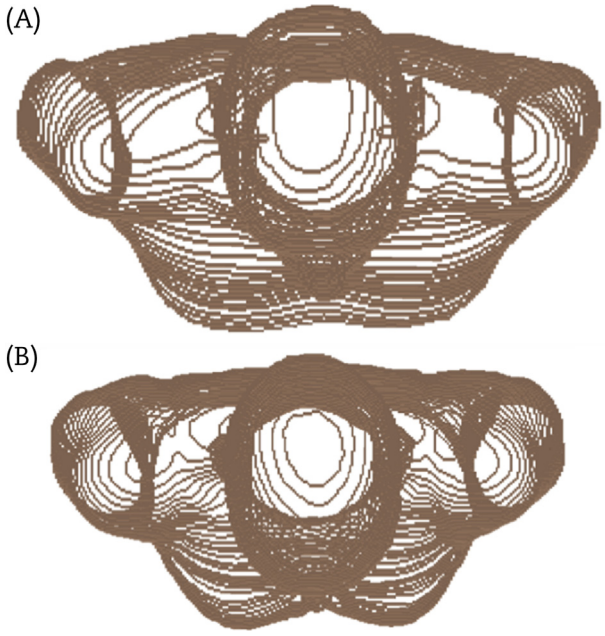

Fig. 1. Skins of International Commission on Radiological Protection (ICRP) reference adult phantoms viewed in superior-inferior direction. (A) male and (B) female.

phantoms. This overestimation also is an issue with all of the other charged particles.

Besides this, there is a more critical limitation; that is, the micron-thick radiosensitive target layer in the skin cannot be represented in voxel phantoms due to the limited voxel resolutions. The basal cells of the epidermis in the human skin are particularly sensitive to radiation with respect to carcinogenesis. The ICRP recommends that a range from 50 μm to 100 μm below the skin surface is an appropriate depth for the basal cell layer of most parts of the skin, and that a depth of 70 μm is a reasonable mean value for practical dose assessment [18–20]. However, the recommended skin target layer cannot be defined in voxel phantoms; thus, skin doses are approximated by calculating absorbed doses averaged over the entire skin of voxel phantoms instead of over the thin target layer. This approximation, for example, was used to calculate the skin DCs of ICRP Publication 116 [18] with respect to the ICRP reference voxel phantoms. Although this approach would be reliable for penetrating radiations (e.g., photons or neutrons), it is no longer reliable for weakly penetrating radiations (e.g., beta or alpha particles) involving a significant dose-distribution gradient in the skin.

Recently, Yeom et al. [21] constructed a set of polygon-mesh (PM)-based skin models by converting the skins of the ICRP reference voxel phantoms into a high-quality PM format; they also included the recommended 50-μm-thick radiosensitive target layer. The PM-based skin models were then directly implemented in a Monte Carlo code, Geant4 [22], to calculate skin DCs for the idealized external beams of electrons, and then the calculated values were compared with the skin DCs of ICRP Publication 116 [18] calculated with the ICRP reference voxel phantoms. It was shown that the calculated skin DCs were significantly different from the ICRP-116 values: the difference was as large as ~7,700 times for electron energies less than 1 MeV, which was considered to be a significant issue for further investigation. Therefore, as an extension of the previous study, the present study calculated the skin DCs for three other particles (i.e., photons, protons, and helium ions) using the PM-based skin models and compared the results with the skin DCs of ICRP Publication 116 [18].

2. Materials and methods

2.1. Skin PM models

Fig. 2 shows the PM-based skin models including the 50-μm-thick target layer developed by Yeom et al. [21] along with the original skin voxel models of the ICRP reference phantoms [2] used to construct the PM-based skin models. It can be seen that the PM-based skin models not only represent smooth and fully-enclosed surfaces, but also maintain the original shapes of the ICRP skin voxel models. The masses of the ICRP skin voxel models (male, 3,728 g and female, 2,721 g) are larger than the reference values (male, 3,300 g and female, 2,300 g) of ICRP Publication 89 [23], whereas those of the PM-based skin models are in accordance with the reference values. Additionally, the average thicknesses of the PM-based skin models are 1.69 mm and 1.33 mm for male and female, respectively, which values are in good agreement with the reference values (male, 1.6 mm; female, 1.3 mm) [2,18]. The inner space of the PM-based skin models is filled with the ICRU-44 adult average soft tissue specified in ICRP Report 46 [24], but with slightly modified densities (male, 1.024 g/cm^3; female, 1.010 g/cm^3) for maintenance of the reference body weights of 73 kg (male) and 60 kg (female).

2.2. Monte Carlo simulation with Geant4

In the present study, to calculate skin DCs for idealized external beams of photons, protons, and helium ions, the PM-based skin models were implemented in the Geant4 Monte Carlo radiation transport code (version 10.01) [22]. In preparation for implementation, the skin models in the PM format were converted to the tetrahedral-mesh format using the TetGen code [25], and the converted tetrahedral-mesh models were implemented in Geant4 using the G4Tet class. Note that the tetrahedralization process did not distort the original shape of the PM-based skin models and significantly improved the computation speed [26].

The skin DCs were calculated for the energies and irradiation geometries considered in ICRP-116 [18]; photons from 10 keV to 10 GeV in antero-posterior (AP), postero-anterior (PA), left-lateral (LLAT), right-lateral (RLAT), rotational (ROT), and ISO geometries; protons from 1 MeV to 10 GeV in AP, PA, LLAT, RLAT, ROT, and ISO geometries; and helium ions from 1 MeV/u to 100 GeV/u in AP, PA, and ISO geometries.

The irradiation geometries were modeled using the G4GeneralParticleSource. The energies deposited to the skin target layer were calculated using the G4PSEnergyDeposit class. The electromagnetic physics library of G4EmLivermorePhysics was used to transport photons and electrons, and the hadronic physics library of G4HadronPhysicsQGSP_BERT_HP was used to transport hadronic particles [27]. Considering the 50-μm-thick target layer, a secondary-range cut value of 1 μm was set for all particles. The number of primary particles for simulation varied within the 10^6–10^9 range according to the type and energy of particles, so as to limit the statistical relative errors to less than 5% for most of the calculation cases. The simulations were performed on the AMD OpteronTM 6176(at 2.3 GHz and 256 GB memory).

3. Results and discussion

3.1. Skin DCs

Fig. 3 plots the skin DCs calculated in this study along with the ICRP-116 skin DCs for photons. It can be seen that the ICRP-116 skin DCs were generally in good agreement with the calculated skin DCs for most of the photon energies. In some energy regions, relatively

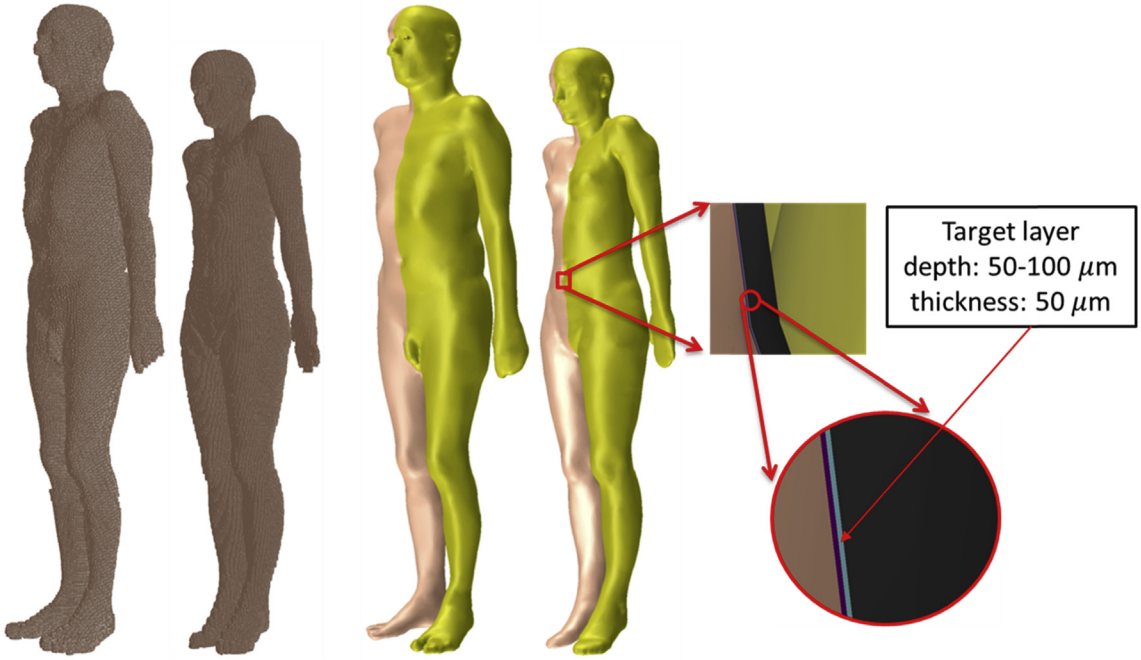

Fig. 2. International Commission on Radiological Protection (ICRP) skin voxel models (left) and polygon-mesh skin models (right).

larger discrepancies were found. For the energies less than 0.03 MeV, the ICRP-116 skin DCs were smaller, with a maximum difference of 133% at 0.01 MeV in the ISO geometry for male. This difference is because these low-energy photon beams establish the maximum dose near the skin surface, the dose value rapidly decreasing with depth by attenuation. For the energies within the range of 0.2–10 MeV, by contrast, the ICRP-116 skin DCs were larger, with a maximum difference of 40% at 1.33 MeV in the AP geometry for males. This reversal phenomenon is due mainly to the fact that these megavoltage photon beams establish a dose build-up region within the skin, in which the minimum dose appears at the skin surface and the dose value increases with depth, establishing the maximum dose at a depth deeper than the skin target layer.

Fig. 4 plots the skin DCs for protons. It can be seen that for high-energy protons (> 10 MeV), the ICRP-116 skin DCs were in good agreement with the skin DCs calculated with the PM models: the differences were all less than 20%. However, there were significant differences for the lower energies. For the very low energies ($\leq$ 1.5 MeV), the skin DCs of the PM models were essentially zero, whereas the ICRP-116 skin DCs showed some positive values. The values of the PM models are reasonable, considering that the low-energy protons, the continuous slowing down approximiation (CSDA) ranges of which are less than 50 μm in skin, cannot penetrate the 50-μm-thick dead-skin layer, thereby demonstrating the significant overestimation of the ICRP-116 skin DCs. By contrast, for higher energies up to 10 MeV, the ICRP-116 skin DCs were significantly underestimated, as large as ~16 times at 3 MeV, which is because that the protons in this energy region penetrate the dead layer and establish a Bragg peak in the target layer.

Fig. 5 plots the skin DCs for helium ions. It can be seen that the general tendency of the difference in skin DCs is similar to that for protons. For the high-energy helium ions ($\geq$ 10 MeV/u), the ICRP-116 skin DCs were in good agreement with the skin DCs of the PM models: the discrepancies were less than 26%. By contrast, significant differences were observed for the lower energies, which include the typical energy range of alpha radiation (4–8 MeV) frequently faced in the field of radiation protection. Except for 1 MeV/u, the ICRP-116 skin DCs were significantly underestimated, i.e., as large as ~16 times at 3 MeV/u, which, again, was due to the establishment of the Bragg peak in the target layer. For 1 MeV/u, the ICRP-116 skin DCs showed significant overestimations relative to the essentially zero values of the calculated skin DCs; this, once again, is because the 1-MeV/u helium ions deposit all of their energies to the skin dead layer, being unable to reach the target layer in the PM models.

3.2. Influence on effective DCs

The present study also investigated how discrepancies in skin dose affect effective dose, the most important protection quantity in radiation protection, which is defined by the following equation:

$$E = \sum_T w_T \sum_R w_R \left(\frac{D_{T,R}^{Male} + D_{T,R}^{Female}}{2} \right)$$

where $D_{T,R}$ is the absorbed dose for tissue T and radiation R, w_T is the tissue-weighting factor, and w_R is the radiation-weighting factor. Note that the tissue- and radiation-weighting factors are given in ICRP Publication 103 [28]. For this investigation, the ICRP-116 effective DCs [18] were compared with the effective DCs calculated by replacing the ICRP-116 skin DCs with the PM-model-calculated skin DCs.

Fig. 6 compares the ICRP-116 effective DCs and the effective DCs calculated in the present study using the PM models for photons. It can be seen that the ICRP-116 effective DCs were in good agreement with the calculated effective DCs for all of the calculation cases, even if some discrepancies in skin DCs were found as shown in Fig. 3. Relatively large discrepancies were found only for the 0.01 MeV photons, the maximum difference being 72% in the PA geometry. This result shows that the skin dose discrepancies do not significantly affect effective doses for photon exposures, which is due to the fact that doses for the other organs and tissues are more important than that for the skin, which has a small tissue-

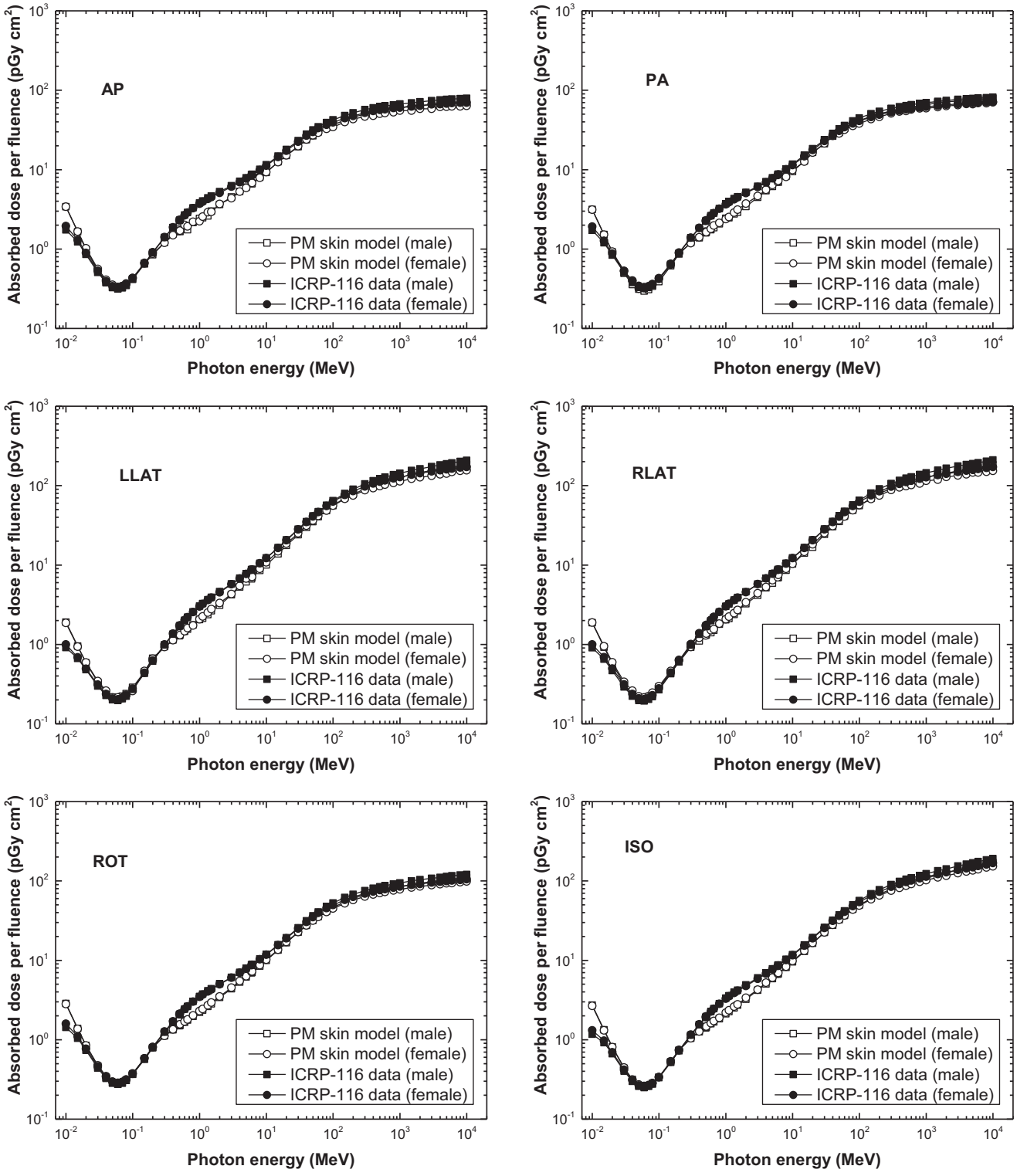

Fig. 3. Skin absorbed dose per fluence (pGy cm^2) for photon exposures in antero-posterior (AP), postero-anterior (PA), left-lateral (LLAT), right-lateral (RLAT), rotational (ROT), and isotropic (ISO) geometries. Polygon-mesh (PM) skin model–target layer: male (unfilled squares) and female (unfilled circles); International Commission on Radiological Protection (ICRP)-116 data–entire skin: male (filled squares) and female (filled circles) [18].

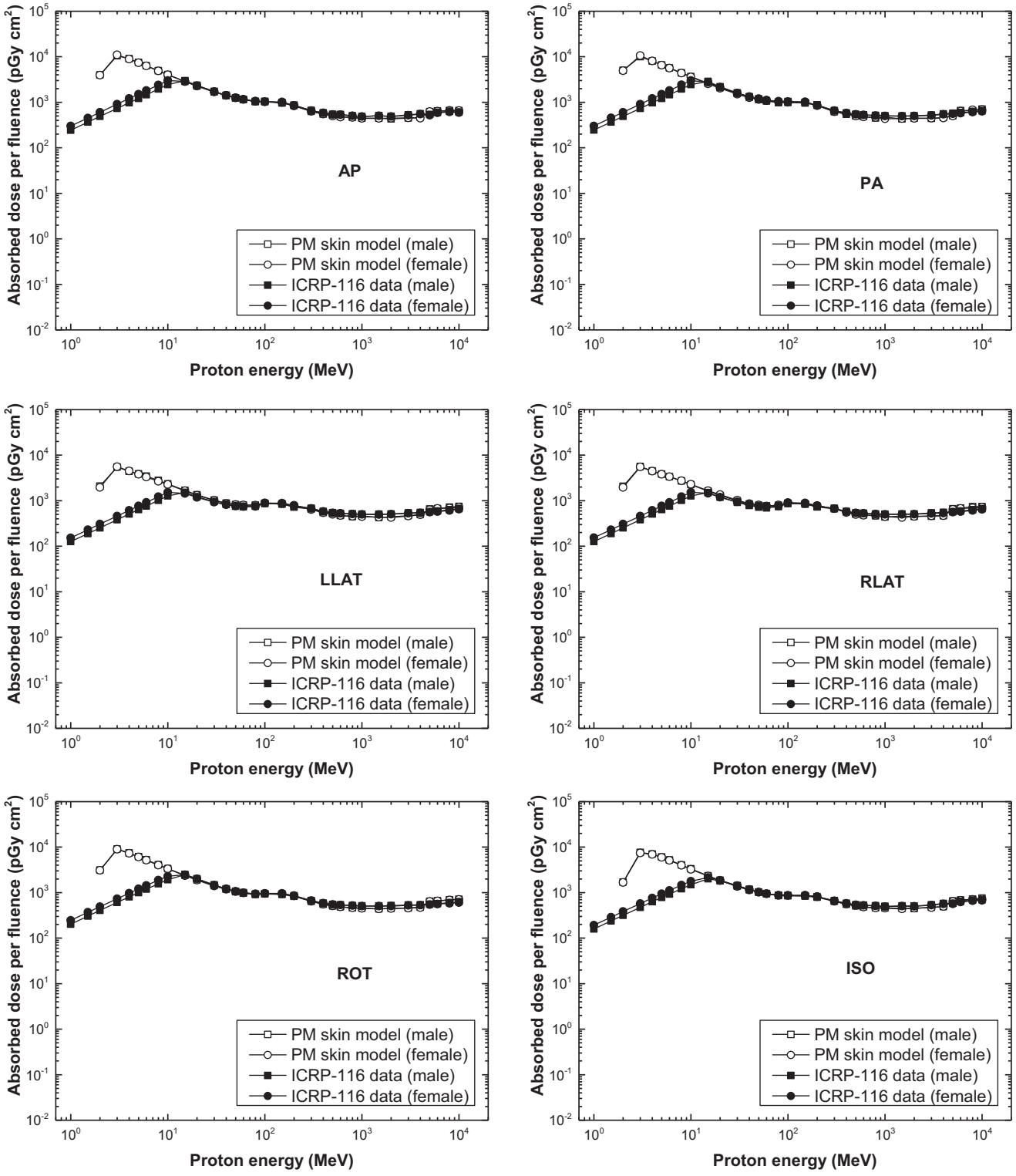

Fig. 4. Skin absorbed dose per fluence (pGy cm^2) for proton exposures in antero-posterior (AP), postero-anterior (PA), left-lateral (LLAT), right-lateral (RLAT), rotational (ROT), and isotropic (ISO) geometries. Polygon-mesh (PM) skin model–target layer: male (unfilled squares) and female (unfilled circles); International Commission on Radiological Protection (ICRP)-116 data–entire skin: male (filled squares) and female (filled circles) [18].

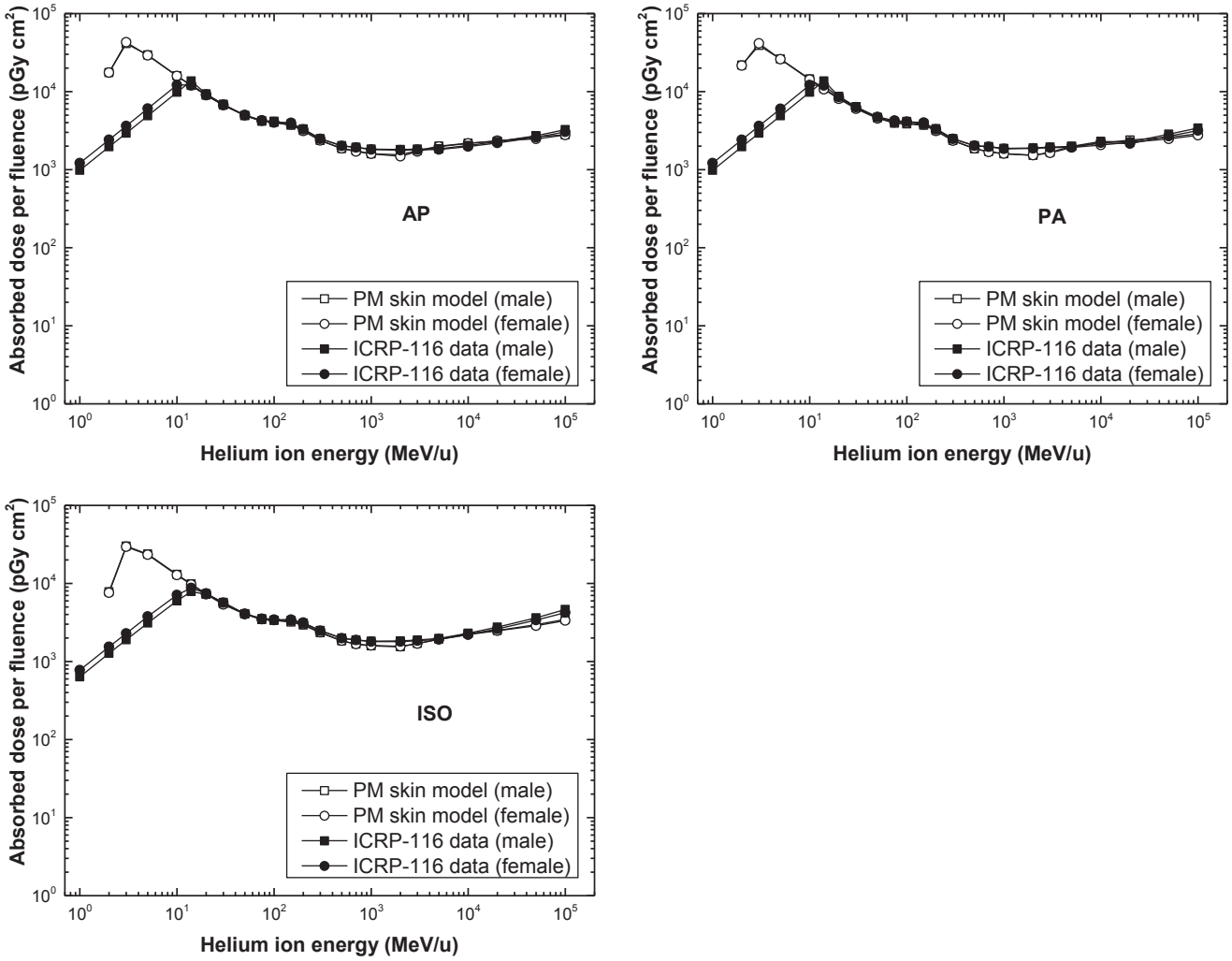

Fig. 5. Skin absorbed dose per fluence (pGy cm^2) for helium ion exposures in antero-posterior (AP), postero-anterior (PA), and isotropic (ISO) geometries. Polygon-mesh (PM) skin model–target layer: male (unfilled squares) and female (unfilled circles); International Commission on Radiological Protection (ICRP)-116 data–entire skin: male (filled squares) and female (filled circles) [18].

weighting factor ($w_T = 0.01$).

Fig. 7 compares the effective DCs for protons. In contrast with the photon results, the ICRP-116 effective DCs were indeed significantly different from the calculated effective DCs for low-energy protons ($\leq$ 10 MeV). This result means that the skin dose discrepancies significantly affect the calculation of effective dose for proton exposures, despite the small tissue weighting factor of the skin ($w_T = 0.01$); this is because these low-energy protons do not penetrate the skin to which most energies are deposited and thus the skin dose is the major factor determining effective dose calculation. This indicates, further, that the ICRP-116 DCs for effective dose are not reliable, underestimating effective dose as much as ~14 times at 3 MeV. Note that, from a conservative point of view, this significant underestimation of effective doses could represent a critical problem in radiological protection.

Fig. 8 compares the effective dose DCs for helium ions. Similarly to the proton results, the ICRP-116 effective DCs were significantly different from the values calculated in the present study for the energies ($\leq$ 10 MeV/u), and also underestimated the effective dose by as much as ~14 times at 3 MeV/u. This result shows, again, that skin dose discrepancies significantly affect effective doses for helium ion exposures.

4. Conclusion

In the present study, the skin DCs for photons, protons, and helium ions were calculated using the PM-based skin models including the 50-μm-thick target layer; results were compared with the ICRP-116 values calculated using the voxel-type ICRP reference phantoms not including the thin target layer. The comparison results showed that for photon exposures, there was good agreement between the skin DCs calculated using the PM models and the ICRP-116 values. By contrast, for the charged particles, there was a significant difference; that is, the ICRP-116 skin DCs were smaller than the values calculated by the PM models by up to ~16 times for both protons and helium ions, meaning that the ICRP-116 skin DCs underestimate the skin DCs by up to ~16 times. These differences in skin dose also significantly affected the calculation of the effective dose (E), which is reasonable, because the skin dose is the major factor determining effective dose calculation for charged particles. The results of the current study, and the previous study on electrons, generally show that the ICRP-116 DCs for skin dose and effective dose are not reliable for charged particles. Although neutrons were not considered in the present study, we believe that they would show behavior similar to that of photons. Recently, the

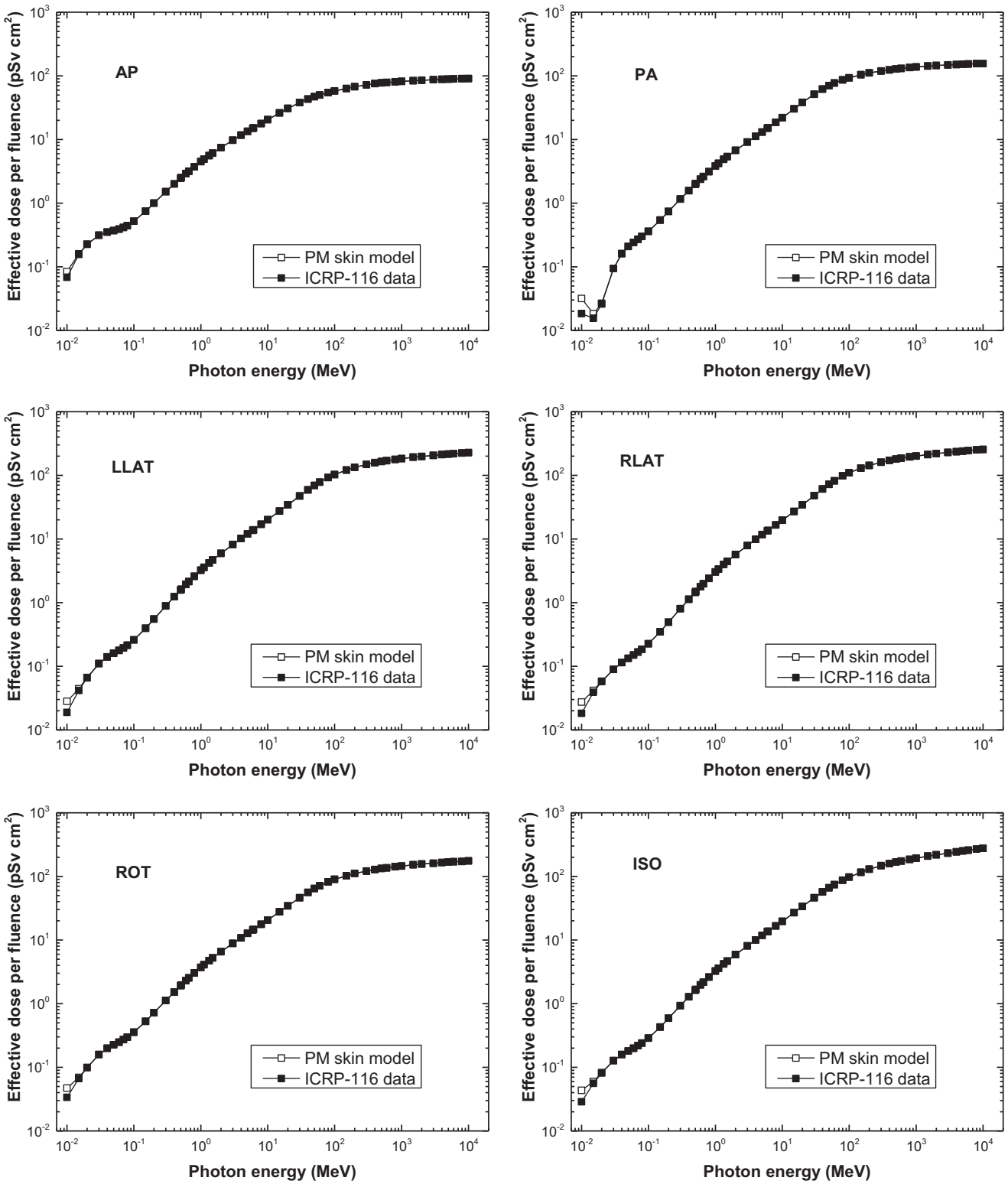

Fig. 6. Effective dose per fluence (pSv cm^2) for photon exposures in antero-posterior (AP), postero-anterior (PA), left-lateral (LLAT), right-lateral (RLAT), rotational (ROT), and isotropic (ISO) geometries. Polygon-mesh (PM) skin model–target layer (unfilled squares) and International Commission on Radiological Protection (ICRP)-116 data–entire skin (filled squares) [18].

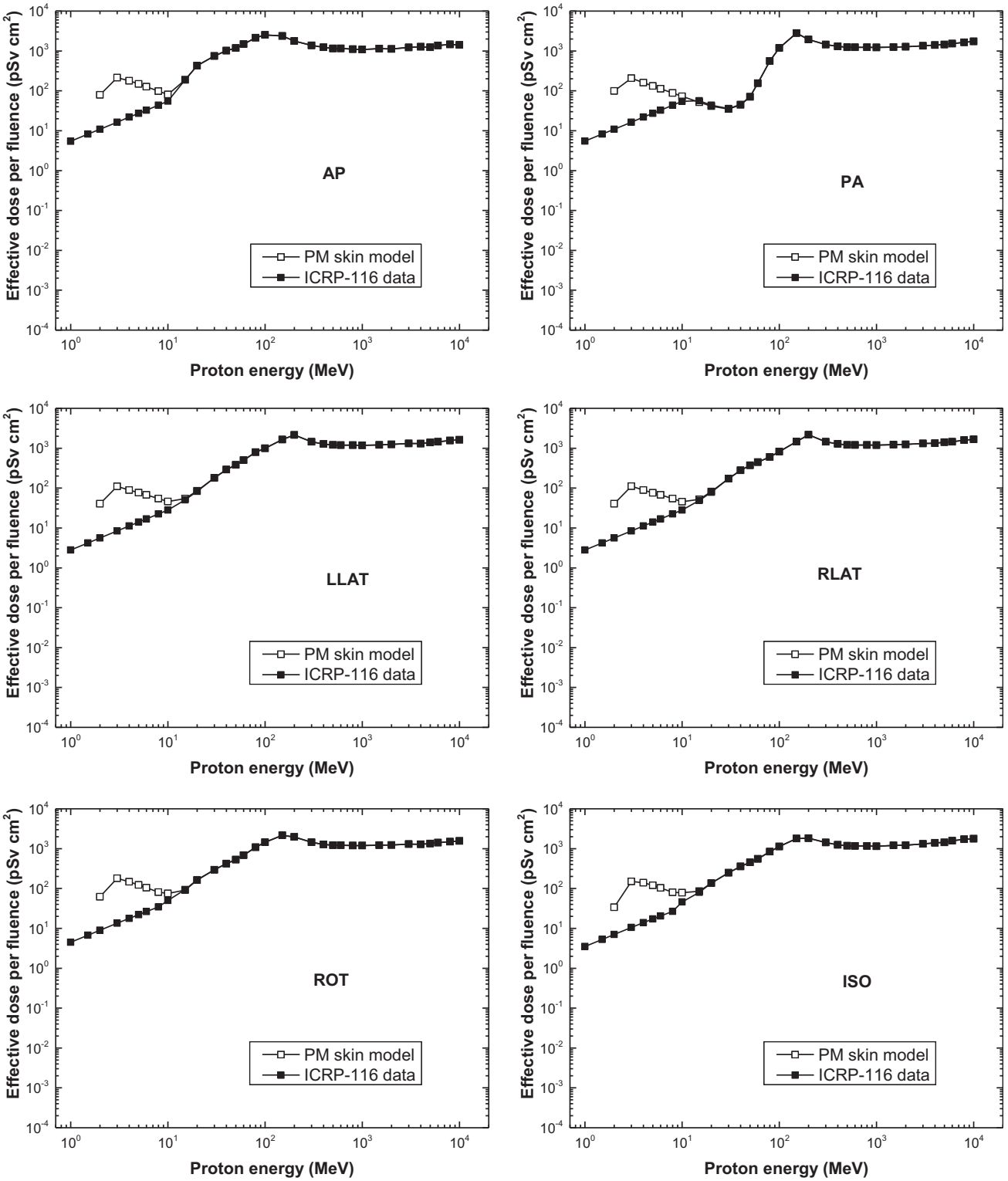

Fig. 7. Effective dose per fluence (pSv cm^2) for proton exposures in antero-posterior (AP), postero-anterior (PA), left-lateral (LLAT), right-lateral (RLAT), rotational (ROT), and isotropic (ISO) geometries. Polygon-mesh (PM) skin model–target layer (unfilled squares) and International Commission on Radiological Protection (ICRP)-116 data–entire skin (filled squares) [18].

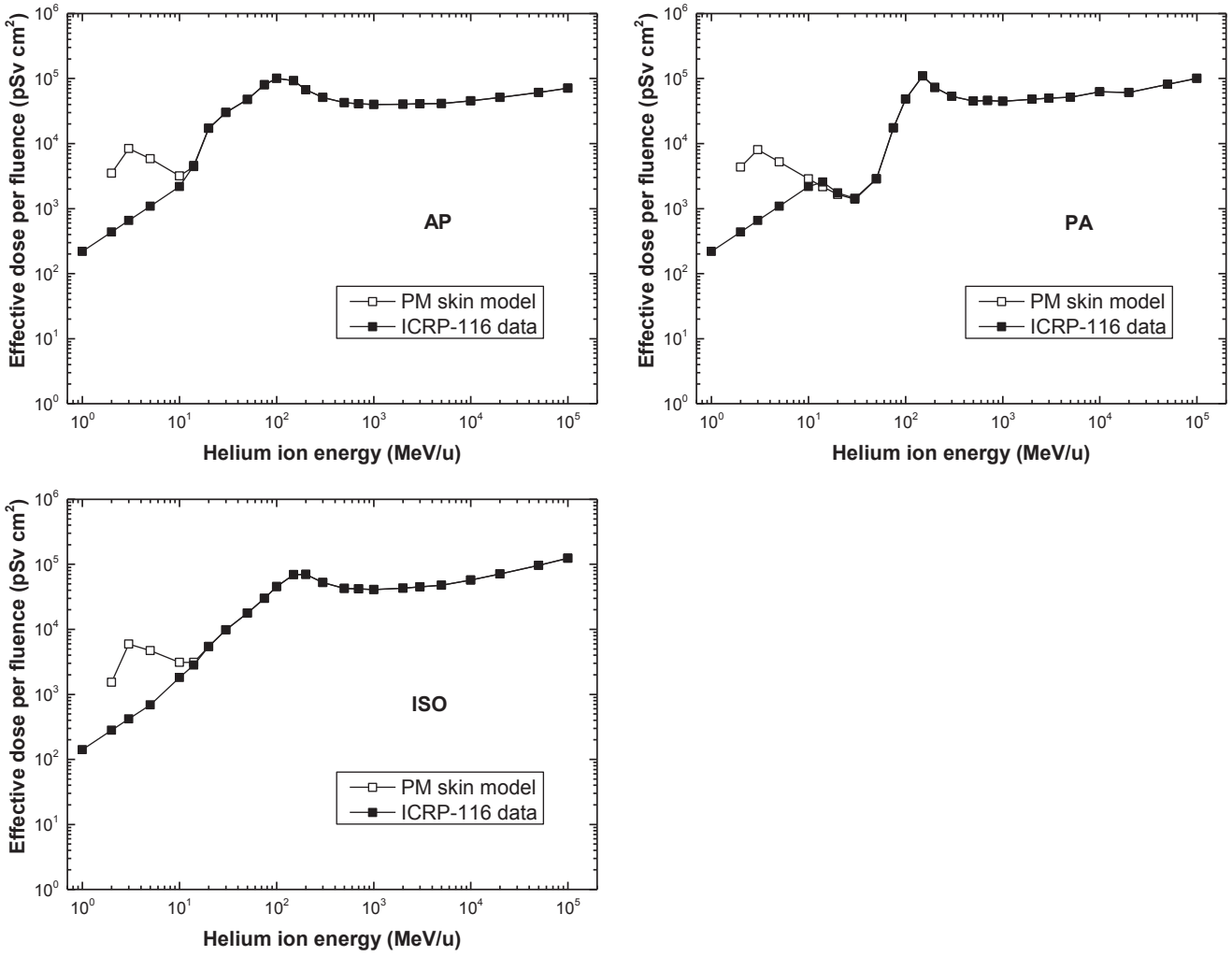

Fig. 8. Effective dose per fluence (pSv cm^2) for helium ion exposures in antero-posterior (AP), postero-anterior (PA), and isotropic (ISO) geometries. Polygon-mesh (PM) skin model–target layer (unfilled squares) and ICRP-116 data–entire skin (filled squares) [18].

ICRP formed a task group (i.e., Task Group 103) to develop a set of mesh-type ICRP reference phantoms to address the limitations of the current voxel-type ICRP reference phantoms. In light of the present study, the Task Group has made a decision to include the 50-μm-thick skin target layer in the new mesh-type reference phantoms.

Conflicts of interest

All authors have no conflicts of interest to declare.

Acknowledgments

This work was supported by the research fund of Hanyang University (HY-2017), by the Nuclear Safety Research and Development (NSR&D) Program through the Korea Foundation of Nuclear Safety (KoFONS) funded by Nuclear Safety and Security Commission (NSSC) (Project Number: 1705006), by the Basic Science Research Program through the National Research Foundation of Korea (NRF) funded by the Ministry of Education (Project Number: NRF-2016R1D1A1A09916337), and by ETRI R&D Program (Development of particle beam range verification technology based on prompt gamma-ray measurements) funded by the Government of Korea (Project Number: 15ZC1810).

References

[1] X.G. Xu, An exponential growth of computational phantom research in radiation protection, imaging, and radiotherapy: a review of the fifty-year history, Phys. Med. Biol. 59 (2014) R233–R302.
[2] International Commission on Radiological Protection (ICRP), Adult Reference Computational Phantoms, vol. 39, ICRP Publication 110, Ann. ICRP, 2009, 165 pages.
[3] A. Pujol, S.J. Gibbs, A Monte Carlo method for patient dosimetry from dental X-ray, Dentomaxillofac. Radiol 11 (1982) 25–33.
[4] M. Zankl, R. Velt, G. Williams, K. Schneider, H. Fendel, N. Petoussi-Henss, G. Drexler, The construction of computer tomographic phantoms and their application in radiology and radiation protection, Radiat. Environ. Biophys 27 (1988) 153–164.
[5] X.G. Xu, T.C. Chao, A. Bozkurt, VIP-Man: an image-based whole-body adult male model constructed from color photographs of the Visible Human Project for multi-particle Monte Carlo calculations, Health Phys. 78 (2000) 476–486.
[6] N. Petoussi-Henss, M. Zankl, U. Fill, D. Regulla, The GSF family of voxel phantoms, Phys. Med. Biol. 47 (2002) 89–106.
[7] C. Lee, D. Lodwick, D. Hasenauer, J.L. Williams, C. Lee, W.E. Bolch, Hybrid computational phantoms of the male and female newborn patient: NURBS-based whole-body models, Phys. Med. Biol. 52 (2007) 3309–3333.
[8] J.H. Jeong, S. Cho, K.W. Cho, C.H. Kim, Deformation of the reference Korean voxel male model and its effect on dose calculation, J. Radiat. Prot. Res. 33 (2008) 167–172.
[9] C.H. Kim, S.H. Choi, J.H. Jeong, C. Lee, M.S. Chung, HDRK-Man: a whole-body voxel model based on high-resolution color slice images of a Korean adult male cadaver, Phys. Med. Biol. 53 (2008) 4093–4106.
[10] J. Zhang, Y.H. Na, P.F. Caracappa, X.G. Xu, RPI-AM RPI-AF a pair of mesh-based, size-adjustable adult male and female computational phantoms using ICRP-89 parameters and their calculations for organ doses from monoenergetic

photon beams, Phys. Med. Biol. 54 (2009) 5885–5908.
[11] V.F. Cassola, V.J. de Melo Lima, R. Kramer, H.J. Khoury, FASH and MASH: female and male adult human phantoms based on polygon mesh surfaces: I. Development of the anatomy, Phys. Med. Biol. 55.1 (2009) 133–162.
[12] C. Lee, D. Lodwick, J. Hurtado, D. Pafundi, J.L. Williams, W.E. Bolch, The UF family of reference hybrid phantoms for computational radiation dosimetry, Phys. Med. Biol. 55 (2010) 339–363.
[13] D. Broggio, J. Beurrier, M. Bremaud, A. Desbree, J. Farah, C. Huet, D. Franck, Construction of an extended library of adult male 3D models: rationale and results, Phys. Med. Biol. 56 (23) (2011) 7659–7692.
[14] M.R. Maynard, J.W. Geyer, J.P. Aris, R.Y. Shifrin, W.E. Bolch, The UF family of hybrid phantoms of the developing human fetus for computational radiation dosimetry, Phys. Med. Biol. 56 (2011) 4839–4879.
[15] S. Park, Y.S. Yeom, J.H. Kim, H.S. Lee, M.C. Han, J.H. Jeong, C.H. Kim, Development of reference Korean organ and effective dose calculation online system, J. Radiat. Prot. Res. 39 (2014) 30–37.
[16] Y.S. Yeom, J.H. Jeong, C.H. Kim, B.K. Ham, K.W. Cho, S.B. Hwang, HDRK-Woman: whole-body voxel model based on high-resolution color slice images of Korean adult female cadaver, Phys. Med. Biol. 59 (14) (2014) 3969–3984.
[17] Y.S. Yeom, M.C. Han, C.H. Kim, J.H. Jeong, Conversion of ICRP male reference phantom to polygon-surface phantom, Phys. Med. Biol. 58 (2013) 6985–7007.
[18] International Commission on Radiological Protection (ICRP), Conversion Coefficients for Radiological Protection Quantities for External Radiation Exposures, vol. 40, ICRP Publication 116, Ann. ICRP, 2010, 257 pages.
[19] International Commission on Radiological Protection (ICRP), Recommendations of the ICRP, vol. 1, ICRP Publication 26, Ann. ICRP, 1977, 53 pages.
[20] International Commission on Radiological Protection (ICRP), Occupational Intakes of Radionuclides: Part 1, vol. 44, ICRP Publication 130, Ann. ICRP, 2015, 188 pages.
[21] Y.S. Yeom, C.H. Kim, T.T. Nguyen, C. Choi, M.C. Han, J.H. Jeong, Construction of new skin models and calculation of skin dose coefficients for electron exposures, J. Korean Phys. Soc. 69 (2016) 512–517.
[22] S. Agostinelli, J. Allisonas, K. Amako, J. Apostolakis, H. Araujo, P. Arce, M. Asai, D. Axen, S. Banerjee, G. Barrand, F. Behner, L. Bellagamba, J. Boudreau, L. Broglia, A. Brunengo, H. Burkhardt, S. Chauvie, J. Chuma, R. Chytracek, G. Cooperman, G. Cosmo, P. Degtyarenko, A. Dell'Acqua, G. Depaola, D. Dietrich, R. Enami, A. Feliciello, C. Ferguson, H. Fesefeldt, G. Folger, F. Foppiano, A. Forti, S. Garelli, S. Giani, R. Giannitrapani, D. Gibin, J.J. Gómez Cadenas, I. González, G. Gracia Abril, G. Greeniaus, W. Greiner, V. Grichine, A. Grossheim, S. Guatelli, P. Gumplinger, R. Hamatsu, K. Hashimoto, H. Hasui, A. Heikkinen, A. Howard, V. Ivanchenko, A. Johnson, F.W. Jones, J. Kallenbach, N. Kanaya, M. Kawabata, Y. Kawabata, M. Kawaguti, S. Kelner, P. Kent, A. Kimura, T. Kodama, R. Kokoulin, M. Kossov, H. Kurashige, E. Lamanna, T. Lampén, V. Lara, V. Lefebure, F. Lei, M. Liendl, W. Lockman, F. Longo, S. Magni, M. Maire, E. Medernach, K. Minamimoto, P. Mora de Freitas, Y. Morita, K. Murakami, M. Nagamatu, R. Nartallo, P. Nieminen, T. Nishimura, K. Ohtsubo, M. Okamura, S. O'Neale, Y. Oohata, K. Paech, J. Perl, A. Pfeiffer, M.G. Pia, F. Ranjard, A. Rybin, S. Sadilov, E. Di Salvo, G. Santin, T. Sasaki, N. Savvas, Y. Sawada, S. Scherer, S. Sei, V. Sirotenko, D. Smith, N. Starkov, H. Stoecker, J. Sulkimo, M. Takahata, S. Tanaka, E. Tcherniaev, E. Safai Tehrani, M. Tropeano, P. Truscott, H. Uno, L. Urban, P. Urban, M. Verderi, A. Walkden, W. Wander, H. Weber, J.P. Wellisch, T. Wenaus, D.C. Williams, D. Wright, T. Yamada, H. Yoshida, D. Zschiesche, GEANT4—a simulation toolkit, Nucl. Instrum. Methods Phys. Res. A 506 (3) (2003) 250–303.
[23] International Commission on Radiological Protection (ICRP), Basic Anatomical and Physiological Data for Use in Radiological Protection Reference Values, vol. 32, ICRP Publication 89, Ann. ICRP, 2002, 265 pages.
[24] G. White, I.J. Wilson, Photon, electron, proton and neutron interaction data for body tissues, ICRU Report 46 (1992).
[25] H. Si, TetGen, a Delaunay-based quality tetrahedral mesh generator, ACM Trans. Math. Softw. 41 (2) (2015), 36 pages.
[26] Y.S. Yeom, J.H. Jeong, M.C. Han, C.H. Kim, Tetrahedral-mesh-based computational human phantom for fast Monte Carlo dose calculations, Phys. Med. Biol. 59.12 (2014) 3173–3185.
[27] D.H. Wright [Internet]. Geant4 Physics Reference Manual, 2016 (9 December), Available from: http://geant4.cern.ch.
[28] International Commission on Radiological Protection (ICRP), The 2007 Recommendations of the International Commission on Radiological Protection, vol. 37, ICRP Publication 103, Ann. ICRP, 2007, 332 pages.